THE DUST-TO-GAS RATIO IN THE SMALL MAGELLANIC CLOUD TAIL

K. D. Gordon[1], C. Bot[2], E. Muller[3], K. A. Misselt[4], A. Bolatto[5], J.-P. Bernard[6], W. Reach[7]
C. W. Engelbracht[4], B. Babler[8], S. Bracker[8], M. Block[4], G. C. Clayton[9], J. Hora[10], R. Indebetouw[11],
F. P. Israel[12], A. Li[13], S. Madden[14], M. Meade[8], M. Meixner[1], M. Sewilo[1], B. Shiao[1], L. J. Smith[1,16],
J. Th. van Loon[15], & B. A. Whitney[17]

ApJ Letters, in press

ABSTRACT

The Tail region of the Small Magellanic Cloud (SMC) was imaged using the MIPS instrument on the Spitzer Space Telescope as part of the SAGE-SMC Spitzer Legacy. Diffuse infrared emission from dust was detected in all the MIPS bands. The Tail gas-to-dust ratio was measured to be 1200 ± 350 using the MIPS observations combined with existing IRAS and HI observations. This gas-to-dust ratio is higher than the expected 500–800 from the known Tail metallicity indicating possible destruction of dust grains. Two cluster regions in the Tail were resolved into multiple sources in the MIPS observations and local gas-to-dust ratios were measured to be ~440 and ~250 suggests dust formation and/or significant amounts of ionized gas in these regions. These results support the interpretation that the SMC Tail is a tidal tail recently stripped from the SMC that includes gas, dust, and young stars.

Subject headings: galaxies: individual (SMC) — galaxies: ISM — dust, extinction

1. INTRODUCTION

Among the nearby galaxies, the Small Magellanic Cloud (SMC) and nearby regions of the Magellanic Bridge represent a unique astrophysical laboratory for interstellar medium (ISM) studies, because of the SMC's proximity ($\sim$60 kpc, Hilditch et al. 2005), low metallicity (1/5-1/8 $Z_\odot$, Russell & Dopita 1992; Rolleston et al. 1999; Lee et al. 2005; Pérez-Montero & Díaz 2005) and tidally-disrupted interaction status (Zaritsky & Harris 2004). The SMC offers a rare glimpse into the physical processes in an environment with a metallicity that is below the threshold of 1/3–1/4 $Z_\odot$ where the properties of the ISM change as traced by the rapid reduc-

tion in the PAH dust mass fractions and dust-to-gas ratios (Engelbracht et al. 2005; Draine et al. 2007). In addition, the SMC is the only local galaxy that has the ultraviolet dust characteristics (lack of 2175 Å extinction bump, Gordon et al. 2003) of starburst galaxies in the local (Calzetti et al. 1994; Gordon et al. 1997) and high-redshift ($2 < z < 4$, Vijh et al. 2003) universe. The Large and Small Magellanic clouds represent the nearest examples of tidally interacting galaxies and the Magellanic Bridge is a clear manifestation of a close encounter of these two galaxies some 200 Myr ago (Zaritsky & Harris 2004).

In particular, the SMC Tail (Fig. 1) represents one of the nearest example of tidally stripped material. We define the SMC Tail as the portion of the Magellanic Bridge that is adjacent to the SMC Wing and has a higher density and metallicity than the rest of Magellanic Bridge. The Magellanic Bridge (which includes the SMC Tail) is a filament of neutral hydrogen, which joins the SMC and LMC over some 15 kpc (McGee & Newton 1986; Stavely-Smith et al. 1998). Harris (2007) found only locally formed, young ($<$200 Myrs) massive stars associated with the SMC Tail. There is a transition in the metallicities between the SMC Tail with 1/5–1/8 $Z_\odot$ and nearby Magellanic Bridge regions (east of the SMC Tail) with 1/20 $Z_\odot$ (Rolleston et al. 1999, 2003; Lee et al. 2005).

The nature of the SMC Tail as a tidally stripped region with only recent star formation makes the detection and measurement of the amount of dust in this region important. Is there dust in this region of low HI column density and metallicity? Is the gas-to-dust ratio the same as the Body/Wing or has the dust been destroyed due the harsh environment in the Tail? Is the gas-to-dust ratio consistent with expectations for the low metallicity (Draine et al. 2007)? The presence of dust in the SMC Tail region has been inferred for select regions from IRAS point sources. The detection and measurement of widespread dust in the SMC Tail requires sensitive far-

[1] STScI, 3700 San Martin Drive, Baltimore, MD 21218
[2] UMR 7550, Centre de Données Astronomique de Strasbourg (CDS), Université Louis Pasteur, 67000 Strasbourg, France
[3] Dept. of Astrophysics, Nagoya Univ., Furo-cho, Chikusa-ku, Nagoya 464-8602, Japan
[4] Steward Observatory, Univ. of Arizona, Tucson, AZ 85721
[5] Dept. of Astronomy, Univ. of Maryland, College Park, MD 20742
[6] CESR, 9 Av du Colonel Roche, 31028, Toulouse, France
[7] IPAC, Caltech, MS 220-6, Pasadena, CA 91125
[8] Dept. of Astronomy, Univ. of Wisconsin-Madison, 475 N. Charter St., Madison, WI 53706
[9] Dept. of Physics & Astronomy, Louisiana State Univ., Baton Rouge, LA 70803
[10] Harvard-Smithsonian, CfA, 60 Garden St., MS 65, Cambridge, MA 02138
[11] Dept. of Astronomy, Univ. of Virginia, P.O. Box 3818, Charlottesville, VA 22903
[12] Sterrewacht Leiden, Leiden University, PO Box 9513, 2300 RA Leiden, The Netherlands
[13] Dept. of Physics & Astronomy, Univ. of Missouri, Columbia MO 65211
[14] Service d'Astrophysique, CEA/Saclay, l'Orme des Merisiers, 91191 Gif-sur-Yvette, France
[15] Astrophysics Group, Lennard-Jones Lab., Keele Univ., Staffordshire ST5 5BG, UK
[16] Dept. of Physics & Astronomy, Univ. College London, Grower St., London WC1E 6BT, UK
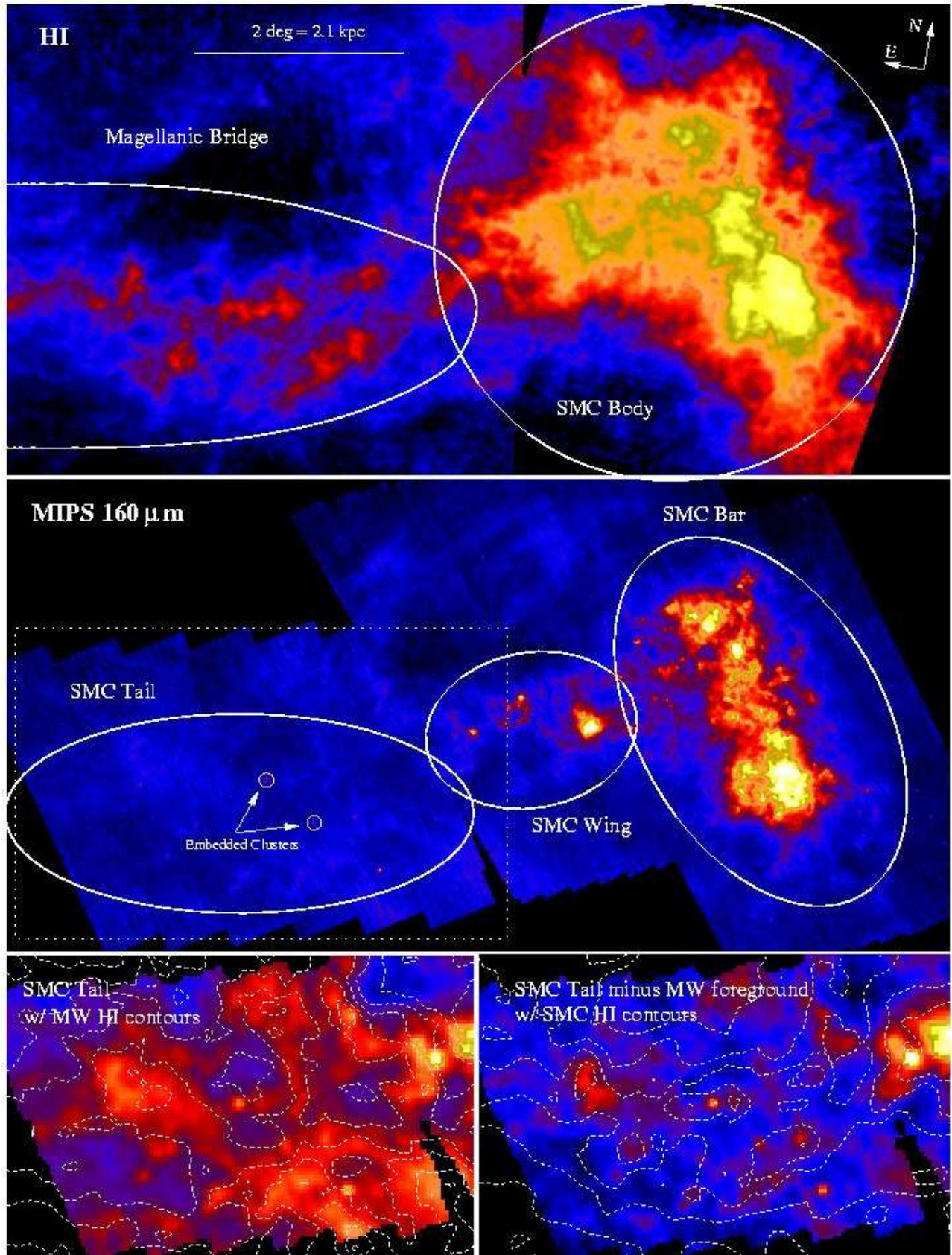[17] Space Sci. Inst., 4750 Walnut St., Suite 205, Boulder, CO 80301

FIG. 1.— The full SMC in HI (top panel) and at 160 μm (middle panel) is shown and various regions are labeled. The dotted box in the middle panel indicates the region shown in the two bottom panels. The left bottom panel shows the 160 μm data convolved to the IRIS-reprocessed IRAS 100 μm resolution (4.'3) overlaid with MW HI contours. The right bottom panel displays the same region after subtraction for the predicted MW foreground cirrus emission. The contours on this panel show the SMC HI measurements. Both bottom panels are displayed on the same scale.

infrared (>100 μm) observations where the bulk of the dust emission occurs.

The SAGE-SMC (Surveying the Agents of Galaxy Evolution in the Tidally-Disrupted, Low-Metallicity Small Magellanic Cloud) Legacy program is using the Spitzer Space Telescope (Werner et al. 2004) to map the SMC from 3.6–160 μm with the Infrared Array Camera (IRAC, Fazio et al. 2004) and the Multiband Imaging Photometer for Spitzer (MIPS, Rieke et al. 2004). The SAGE-SMC observations cover ~30 $\Box^\circ$ and builds on the existing S^{3}MC (Bolatto et al. 2007) observations of the central ~3 $\Box^\circ$. The SAGE-SMC observations consist of two complete maps taken in two epochs. The full details of the entire SAGE-SMC program are given by Gordon et al. (in prep.). This Letter presents the analysis of the SAGE-SMC epoch 1 MIPS observations of the SMC Tail region.

2. DATA

The MIPS observations at 24, 70, and 160 μm were taken on 15-23/9/2007 split into 22 separate maps. Each map consisted of fast rate scan legs with a cross scan offset of 148″ and lengths optimized for each map. We used the MIPS Data Analysis Tool v3.06 (Gordon et al. 2005) to do the basic processing and final mosaicking of the individual images. Extra processing steps were carried out similar to those for SAGE-LMC (Meixner et al. 2006). The epoch 1 SAGE-SMC MIPS 160 μm observations are shown in Fig. 1 along with the integrated HI column density for the same region (Stanimirović et al. 1999; Muller et al. 2003a). The MIPS 70 and 160 μm mosaics were supplemented in SMC Body region with the S^{3}MC data (Bolatto et al. 2007). The full details of the SAGE-SMC processing are given by Gordon et al. (in prep.).

We also used the IRIS reprocessing of the 60 and 100 μm IRAS images (Miville-Deschênes & Lagache 2005) of the same region for our analysis. We convolved the MIPS images to the same resolution as the IRIS-reprocessed IRAS 100 μm image (FWHM = 4.′3) using kernels created in the manner described in (Gordon et al. 2008).

Emission from Milky Way (MW) foreground cirrus clouds dominates the emission seen in the MIPS 160 μm band in the SMC Tail region. This is clearly seen in Fig. 1 in the lower left panel where the 160 μm image is shown with contours from the integrated MW velocity HI gas (Muller et al. 2003a) overplotted. The MIPS 160 μm and MW HI gas emission are well correlated. As was done for the LMC (Bernard et al. 2008), the MW HI gas emission can be used to quantitatively predict the MW dust emission that can then be subtracted from the observed MIPS 160 μm (and other IR bands). This reveals the SMC dust emission and is illustrated in the lower right panel of Fig. 1 showing the MW foreground subtracted MIPS 160 μm image of the SMC Tail region overlaid with the contours from the integrated SMC velocity HI gas (Muller et al. 2003a) overplotted.

3. RESULTS

The presence of dust in the SMC Tail region can be inferred from Fig. 1 (bottom right panel). Quantifying the amount of dust can be done by correlating the MW foreground corrected SMC IR emission with the SMC HI

TABLE 1
INFRARED TO HI SLOPES

Band	MW[a]	SMC Tail
	[MJy sr^{-1} (10^{20} atoms cm^{-2})$^{-1}$]	
IRAS 60	0.129	0.0048 ± 0.0010
MIPS 70	0.191	0.0067 ± 0.0020
IRAS 100	0.522	0.016 ± 0.0032
MIPS 160	0.971	0.053 ± 0.011

[a] Adopted from Bernard et al. (2008).

column densities. Such correlations are shown in Fig. 2 for the MIPS 70 and 160 μm and IRAS 60 and 100 μm bands. The MW foreground IR emission was subtracted from the images by scaling the MW HI image using the coefficients given in Table 1. There is a clear correlation between these IR emissions and the SMC HI column densities at each wavelength and the slopes of these correlations are given in Table 1. The point sources in the IR images were removed using standard sigma clipping to avoid biasing the measurement of the IR to HI correlation. The slopes and formal uncertainties were computed using two different methods that produced consistent results. To account for uncertainties in the foreground IR emission subtraction and absolute calibrations, we have conservatively set the slope uncertainties to 20% for all but the MIPS 70 μm band where the uncertainty is 30% to account for the use of the smaller region. These uncertainties are well above the formal uncertainties in the correlation fits.

The SMC Tail HI gas-to-dust ratio can be computed from the IR to HI slopes assuming a dust grain model. The 60 and 70 μm emission can include contributions from non-equilibrium emission processes (Bernard et al. 2008) and so we only use the 100 and 160 μm correlations to determine the dust temperature. We compute a dust temperature of 15 ± 1.1 K using a black body modified by the emissivity of silicate grains ($\propto \lambda^{-2}$, Weingartner & Draine 2001). Including the 60 and 70 μm correlations increases the temperature to 21 K clearly indicating significant non-equilibrium emission at these wavelengths. The computed HI gas-to-dust ratio is 1200 ± 350 using T = 15 K. For reference, this method gives a HI gas-to-dust ratio of 84 for the MW slopes given by Boulanger et al. (1996) (interpolating to get the 160 μm slope). This MW gas-to-dust ratio is similar to the standard 100-110 value (Sofia & Meyer 2001b,a; Bot et al. 2007; Draine et al. 2007). We adopted a MW reference value of 100, the SMC Tail HI gas-to-dust ratio is $(12 \pm 3.5)\times$ higher than the MW ratio. An analysis using the method of Bot et al. (2004) gives a HI gas-to-dust ratio that is $12\times$ MW. This factor is higher than the expected gas-to-dust ratio value of 5-8$\times$ MW for a metallicity that is 1/5-1/8 solar (Draine et al. 2007). It is very unlikely that this discrepancy between the measured and expected ratio is due to not accounting for the molecular gas component. The gas in the SMC Tail region has a measured molecular-to-atomic ratio of 0.002 (Mizuno et al. 2006).

3.1. *Embedded Clusters*

There are two regions of enhanced, extended emission at 160 μm in the SMC Tail region. These two regions
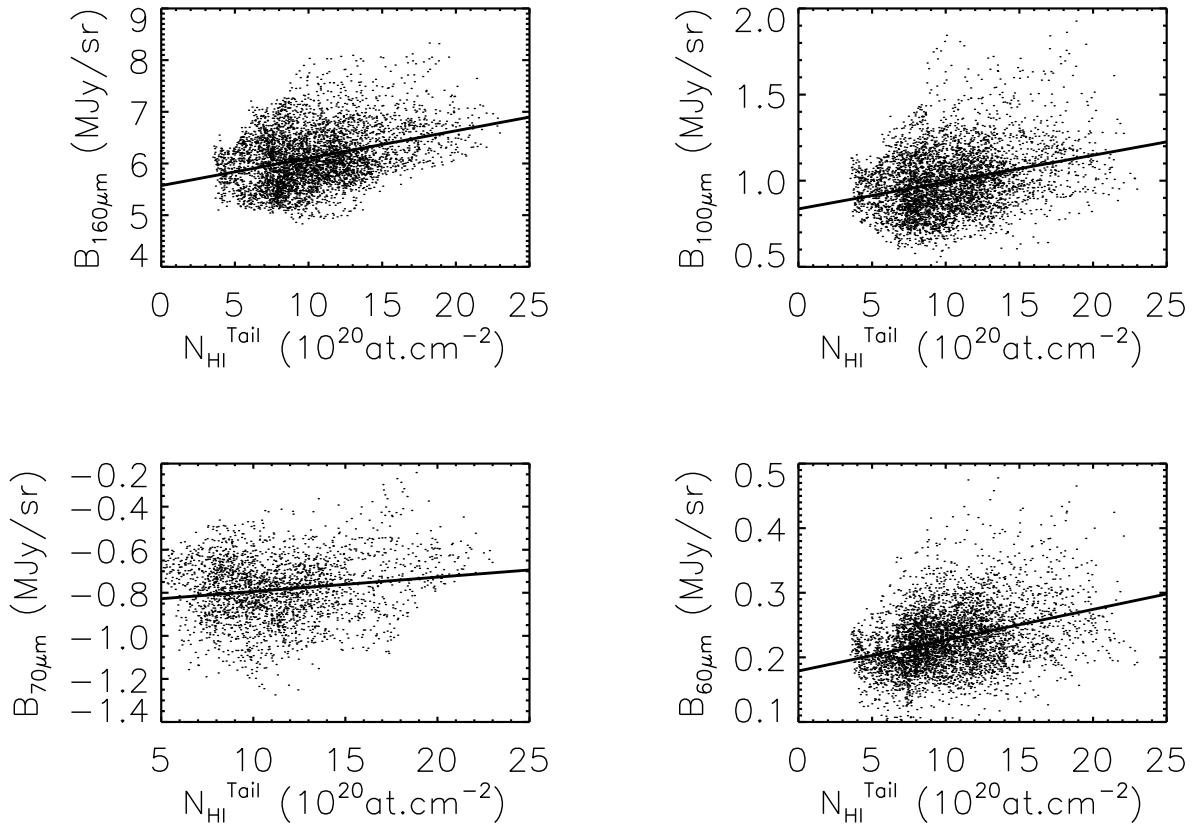
FIG. 2.— The correlation between HI column in the Tail region, N_{HI}^{Tail}, and the MW foreground subtracted MIPS/IRAS surface brightness is shown. The solid line gives the best fit linear correlation. The region over which the correlation is done was restricted to that labeled SMC Tail in Fig. 1 except at MIPS 70 μm. The MIPS 70 μm correlation was done in a smaller region centered on the full region to avoid having the instrumental residuals bias the resulting correlation. The negative 70 μm surface brightnesses are artifacts of the processing for this band where a smoothly varying background (in time) is subtracted for each 70 μm pixel to remove variations in the detector baseline. The significantly larger scatter of the MIPS 70 μm points, as compared to the IRAS 60 μm points, is an indication there still are significant residual MIPS 70 μm instrumental signatures at these low surface brightness levels.

are resolved into multiple sources in all the MIPS bands. The locations of these embedded clusters are shown in Fig. 1 and closeups of the clusters are shown in Fig. 3. The locations of known clusters (Westerlund & Glaspey 1971; Bica & Schmitt 1995) in these regions are shown on archival GALEX far-ultraviolet images. The simultaneous presence of far-UV and far-IR emission indicates young, embedded star forming regions. These cluster regions also have strong Hα emission (Muller & Parker 2007) providing the indication that they harbor massive star formation. The IR stellar properties of these clusters will be investigated in more detail in Chen et al. (in prep.).

These embedded clusters are a clear indication of very recent star formation and provide probes of the local gas-to-dust ratio. The dust mass in each cluster was determined from IR fluxes given in Table 2. The IR fluxes were measured using using an aperture with a radius of $6.'67 \sim 116$ pc and a sky annulus with min/max radii of $8.'33/11.'67$. The uncertainties were calculated using the measured noise in the sky annulus. The dust masses were determined by fitting a two component (warm and cold silicates) grain model to the IR fluxes (Marleau et al. 2006). The cold silicate (which dominates the dust mass)

TABLE 2
CLUSTER PROPERTIES

Property	Region 1	Region 2
RA(2000)	01 56 49	01 49 34.39
DEC(2000)	-74 16 24	-74 38 12
MIPS 24 [Jy]	0.153 ± 0.017	0.062 ± 0.005
IRAS 25 [Jy]	0.215 ± 0.005	0.187 ± 0.007
IRAS 60 [Jy]	3.47 ± 0.05	1.19 ± 0.02
MIPS 70 [Jy]	4.94 ± 0.02	2.15 ± 0.01
IRAS 100 [Jy]	5.80 ± 0.03	2.81 ± 0.008
MIPS 160 [Jy]	9.60 ± 0.01	5.08 ± 0.005
Dust Temp. [K]	$16.5^{+3.5}_{-2.0}$	$17.5^{+4.4}_{-2.5}$
Dust Mass [M$_\odot$]	320^{+700}_{-150}	120^{+290}_{-90}
HI Mass [M$_\odot$]	8.0×10^4	2.2×10^4
HI Gas/Dust	250^{+220}_{-170}	183^{+553}_{-126}
H2 Mass [M$_\odot$]	7×10^3	1×10^3
(HI+H2) Gas/Dust	~ 440	~ 250

dust temperatures and corresponding dust masses are given in Table 2 along with the HI masses determined using the same aperture. Employing the the same analysis described above for the SMC Tail yields dust masses similar to those in Table 2. The HI gas-to-dust ratios are smaller than for the whole SMC Tail, suggesting lo-
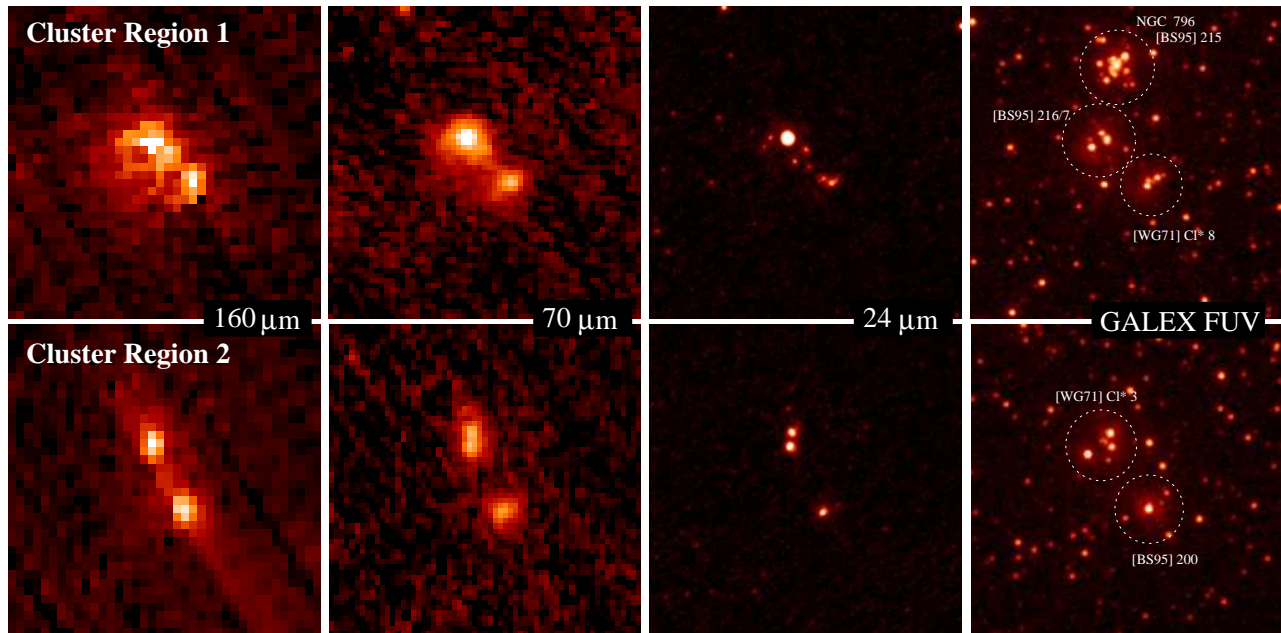
FIG. 3.— The IR appearance of the two embedded clusters is shown for $10' \times 10'$ regions. These two regions correspond to regions C and B of Mizuno et al. (2006). In addition, the GALEX far-UV images of the same regions are shown illustrating the young nature of these objects. The streaking seen in the 160 μm and (to a lesser extent) 70 μm images are residual instrument artifacts.

cal dust enhancements. One alternate explanation for the lower gas-to-dust ratio would be a variable molecular gas content in the SMC Tail region. Adding the H_2 contribution from the measured CO fluxes (Muller et al. 2003b; Mizuno et al. 2006), adjusted for a more appropriate CO-to-H_2 conversion ratio Israel (1997), gives total gas-to-dust ratios (Table 2) that are still below that measured for the whole SMC Tail.

4. SUMMARY/DISCUSSION

We have detected the diffuse infrared emission from dust in the SMC Tail portion of the Magellanic Bridge using the epoch 1 MIPS SAGE-SMC Spitzer Legacy observations. The gas-to-dust ratio in the SMC Tail region was measured to be 1200 ± 350, $(12 \pm 3.5) \times$ MW value, using correlations between the infrared emission and HI column densities. This value is in reasonable agreement with the range of measured SMC Body gas-to-dust ratios (5-11$\times$ MW, Gordon et al. 2003; Bot et al. 2007; Leroy et al. 2007) determined from UV extinction and IR emission measurements. This is consistent with the picture that the SMC Tail has been recently stripped from the SMC Body during a tidal encounter (Connors et al. 2006) and evidence that the gas and dust in the SMC Tail have not been stripped from the LMC or are due to infalling material from the inter-galactic medium. Looking more closely, our infrared measured SMC Tail gas-to-dust ratio is higher than the SMC Body gas-to-dust ratio of 7$\times$ MW (Leroy et al. 2007) that was determined using IR emission measurements and a similar method. In addition, the SMC gas-to-dust ratio of 12$\times$ MW is higher than the expected value from of 5-8$\times$ MW (Draine et al.

2007) for the 1/5-1/8 solar metallicity of the SMC Tail region (Lee et al. 2005). This may indicate there has been destruction of the dust in the SMC Tail or that there is colder dust that is not detected by the MIPS 160 μm observations. Possible plausible dust destruction mechanisms include a harder radiation field due to less dust shielding and shocks due to the tidal interaction (Jones et al. 1996).

Two cluster regions are detected in the MIPS observations indicating the presence of young, embedded star formation. The local gas-to-dust ratio was measured for these two regions to be 2.5–4.4$\times$ MW. These ratios are lower than the gas-to-dust ratio measured for the entire SMC Tail (12$\times$ MW) and lower than that expected for the metallicity of the SMC Tail (5-8$\times$ MW). This suggests there has been dust formation and/or a significant amount of ionized gas is present in these regions. As both regions harbor known HII regions (Muller & Parker 2007), the latter is clearly part of the answer.

This letter presents the detection of dust in the SMC Tail and a preliminary analysis of its dust-to-gas ratio. A more complete analysis of the dust in the whole SMC (Bar, Wing, and Tail) will be presented by Bot et al. (in prep.).

REFERENCES

Bernard, J.-P., et al. 2008, AJ, 136, 919
Bica, E. L. D. & Schmitt, H. R. 1995, ApJS, 101, 41
Bolatto, A. D., et al. 2007, ApJ, 655, 212
Bot, C., et al. 2004, A&A, 423, 567
—. 2007, A&A, 471, 103
Boulanger, F., et al. 1996, A&A, 312, 256
Calzetti, D., Kinney, A. L., & Storchi-Bergmann, T. 1994, ApJ, 429, 582

Connors, T. W., Kawata, D., & Gibson, B. K. 2006, MNRAS, 371, 108

Draine, B. T., et al. 2007, ApJ, 663, 866

Engelbracht, C. W., et al. 2005, ApJ, 628, L29

Fazio, G. G., et al. 2004, ApJS, 154, 10

Gordon, K. D., Calzetti, D., & Witt, A. N. 1997, ApJ, 487, 625

Gordon, K. D., et al. 2003, ApJ, 594, 279

—. 2008, ApJ, 682, 336

—. 2005, PASP, 117, 503

Harris, J. 2007, ApJ, 658, 345

Hilditch, R. W., Howarth, I. D., & Harries, T. J. 2005, MNRAS, 357, 304

Israel, F. P. 1997, A&A, 328, 471

Jones, A. P., Tielens, A. G. G. M., & Hollenbach, D. J. 1996, ApJ, 469, 740

Lee, J.-K., et al. 2005, A&A, 429, 1025

Leroy, A., et al. 2007, ApJ, 658, 1027

Marleau, F. R., et al. 2006, ApJ, 646, 929

McGee, R. X. & Newton, L. M. 1986, Proceedings of the Astronomical Society of Australia, 6, 471

Meixner, M., et al. 2006, AJ, 132, 2268

Miville-Deschênes, M.-A. & Lagache, G. 2005, ApJS, 157, 302

Mizuno, N., et al. 2006, ApJ, 643, L107

Muller, E. & Parker, Q. A. 2007, Publications of the Astronomical Society of Australia, 24, 69

Muller, E., et al. 2003a, MNRAS, 339, 105

Muller, E., Staveley-Smith, L., & Zealey, W. J. 2003b, MNRAS, 338, 609

Pérez-Montero, E. & Díaz, A. I. 2005, MNRAS, 361, 1063

Rieke, G. H., et al. 2004, ApJS, 154, 25

Rolleston, W. R. J., et al. 1999, A&A, 348, 728

—. 2003, A&A, 400, 21

Russell, S. C. & Dopita, M. A. 1992, ApJ, 384, 508

Sofia, U. J. & Meyer, D. M. 2001a, ApJ, 558, L147

—. 2001b, ApJ, 554, L221

Stanimirović, S., et al. 1999, MNRAS, 302, 417

Stavely-Smith, L., et al. 1998, in Reviews in Modern Astronomy, Vol. 11, Reviews in Modern Astronomy, ed. R. E. Schielicke, 117

Vijh, U. P., Witt, A. N., & Gordon, K. D. 2003, ApJ, 587, 533

Weingartner, J. C. & Draine, B. T. 2001, ApJ, 548, 296

Werner, M. W., et al. 2004, ApJS, 154, 1

Westerlund, B. E. & Glaspey, J. 1971, A&A, 10, 1

Zaritsky, D. & Harris, J. 2004, ApJ, 604, 167